



HAL
open science

Charge multiplication effect in thin diamond films

N. Skukan, V. Grilj, I. Sudić, Michal Pomorski, W. Kada, T. Makino, Y. Kambayashi, Y. Andoh, S. Onoda, S. Sato, et al.

► **To cite this version:**

N. Skukan, V. Grilj, I. Sudić, Michal Pomorski, W. Kada, et al.. Charge multiplication effect in thin diamond films. *Applied Physics Letters*, 2016, 109 (4), pp.043502. 10.1063/1.4959863 . hal-01869601

HAL Id: hal-01869601

<https://hal.science/hal-01869601v1>

Submitted on 27 Jun 2023

HAL is a multi-disciplinary open access archive for the deposit and dissemination of scientific research documents, whether they are published or not. The documents may come from teaching and research institutions in France or abroad, or from public or private research centers.

L'archive ouverte pluridisciplinaire **HAL**, est destinée au dépôt et à la diffusion de documents scientifiques de niveau recherche, publiés ou non, émanant des établissements d'enseignement et de recherche français ou étrangers, des laboratoires publics ou privés.

Charge multiplication effect in thin diamond films

N. Skukan^{1,a)}, V. Grilj¹, I. Sudić¹, M. Pomorski², W. Kada³, T. Makino⁴, Y. Kambayashi³, Y. Andoh³, S. Onoda⁴, S. Sato⁴, T. Ohshima⁴, T. Kamiya⁴, M. Jakšić¹

¹*Division of Experimental Physics, Ruđer Bošković Institute, 10000 Zagreb, Croatia*

²*CEA-LIST, Diamond Sensors Laboratory, Gif-sur-Yvette F-91191, France*

³*Division of Electronics and Informatics, Faculty of Science and Technology, Gunma University, Kiryu, Gunma 376-8515, Japan*

⁴*National Institutes for Quantum and Radiological Science and Technology, Takasaki, Gunma 370-1292, Japan*

Abstract

We report herein the enhanced sensitivity for the detection of charged particles in single crystal chemical vapour deposition (scCVD) diamond radiation detectors. The experimental results demonstrate charge multiplication in thin planar diamond membrane detectors, upon impact of 18 MeV O ions, under high electric field conditions. Avalanche multiplication is widely exploited in devices such as avalanche photo diodes, but has never before been reproducibly observed in intrinsic CVD diamond. Because enhanced sensitivity for charged particle detection is obtained for short charge drift lengths without dark counts, this effect could be further exploited in the development of sensors based on avalanche multiplication and radiation detector with extreme radiation hardness

Keywords: diamond, charge multiplication, avalanche, impact ionization

^{a)} **Author to whom correspondence should be addressed. Electronic mail: nskukan@irb.hr.**

30 Because of its extraordinary physical characteristics, synthetic single crystal diamond is a
31 promising material for future applications in various fields such as mechanics, optics and thermal
32 management as well as power electronics and radiation detection. Particularly, radiation detectors
33 based on scCVD diamonds can be found as beam profile monitors for both X-rays and high energy
34 ions, dosimeters for radiotherapy and possible replacements for future upgrades of Atlas and CMS
35 detectors because of their superior radiation hardness [1]. Electrical fields applied to scCVD
36 diamond detectors are typically within a range from 0.1 to approximately 10 V/ μm and most of the
37 literature on charge carrier transport exploit even lower ranges of electric fields rarely reaching 2
38 V/ μm [2, 3]. Values above these are seldom used because of the evolution of erratic leakage
39 currents, causing an increase in noise and eventually an uncontrolled breakdown of the device.
40 Although the theoretical dielectric strength of diamond material is extremely high, real samples
41 suffer from dielectric breakdown at much lower electric field values [4].

42 A possible explanation for the discrepancies between the expected theoretical values and the
43 experimentally used electric fields may lie in the structural defects within the diamond crystal
44 lattice, potentially leading to a significant decrease of the high initial theoretical breakdown voltage
45 [5]. Another practical explanation is that even for a relatively thin 100 μm thick detector, an electric
46 field of 100 V/ μm requires a 10 kV bias voltage. Higher voltages are often not feasible and lead to
47 discharges through vacuum feedthroughs, cables and surface currents on the device. However,
48 possible avalanche multiplication which may be achievable at even higher electric fields, remains
49 a physical effect of great interest to the electronic industry focused on diamond material. Proper
50 knowledge of multiplication parameters will aid in the design of high voltage devices to optimize
51 their geometry, doping and operating parameters. Furthermore, diamond detectors based on the
52 avalanche principle are insensitive or less sensitive to visible light, which may be of great interest
53 for sensor development and scientific community. Therefore, proper knowledge of the parameters
54 ruling the avalanche process is desirable.

55 Charge multiplication in diamond has been tested by multiple groups on a variety of devices [6-9]
56 with diverse results. However, none of these measurements were performed in intrinsic CVD
57 diamond and only one addressed pulse mode multiplication, although the integration time used by
58 the readout electronics did not exclude the photoconductive gain mechanism.

59 To avoid, or at least minimize the possibility of uncontrolled dielectric breakdown while measuring
60 impact ionization multiplication in diamond, the device must be as thin as practically possible,
61 preferably a film. To minimize the total number of defects, the active volume should also be
62 minimized, i.e., the area under the electrodes must be small.

63 Following the development of a thin diamond membrane detector [10, 11], we tested its voltage
64 holding capability and achieved 40 V/ μm before erratic leakage current developed. The tested
65 device was a 3.2 μm thick membrane with 2x2 mm² area contacts. Although this electric field is
66 already the highest applied for diamond radiation detectors, according to the theoretical
67 calculations [12], at least 100 V/ μm is needed to reach an amplification of only 5% and detector

68 thickness of several μm . Therefore, we decided to design a device of the same thickness, but with
69 very minimal contact overlap.

70 The device under investigation was fabricated from standard grade (<1 ppm N concentration),
71 single crystal, $\langle 1\ 0\ 0 \rangle$ oriented CVD diamond produced by Element Six [13]. The sample was
72 mechanically polished down to a $30\ \mu\text{m}$ plate by Almax EasyLab [14]. Further thinning of the
73 central portion of the sample to $3\ \mu\text{m}$ was performed using an Ar/O plasma etching technique
74 described in detail elsewhere [10]. A $300\ \mu\text{m}$ wide Al strip electrode was sputtered on each side of
75 the diamond membrane in a cross-like parallel plate geometry, resulting in a small overlap area of
76 $300 \times 300\ \mu\text{m}^2$ (Figure 1). The placement of the electrodes was carefully chosen under a high
77 magnification optical microscope with birefringence imaging in a membrane region showing no
78 evidence of bulk structural defects (birefringence contrast) or surface defects (pits) arising from
79 polishing. Additionally, having such a small active area is beneficial for reducing the capacitance
80 of the device, resulting in a higher bandwidth for fast transient current measurements. The sample
81 was glued onto a specially designed printed circuit board with a via-hole in the central area to
82 contain the transmission detector. An SMA connector was soldered to the board near the
83 membrane. The top strip electrode was connected to the central pin of the SMA connector by $60\ \mu\text{m}$
84 thick golden wire and silver-loaded conductive paste. The back strip electrode was grounded.
85 In such a configuration the capacitance of the detector was estimated to be less than $0.5\ \text{pF}$. The
86 thickness of the detector was estimated from the energy loss measurements using a telescope
87 configuration with a silicon surface barrier E detector behind the diamond transmission detector,
88 DeltaE. The final thickness of scCVD diamond membrane was measured to be $3.25 \pm 0.1\ \mu\text{m}$ in the
89 area of interest.

90 Prior to irradiation, dark I-V characteristics of the diamond detector were measured to assure the
91 dielectric strength and absence of hard break-down. The device showed no leakage current ($I < 100$
92 fA) up to $\pm 500\ \text{V}$ ($154\ \text{V}/\mu\text{m}$). The device was not tested to the maximum voltage applied in later
93 measurements to avoid hard breakdown before obtaining the data

94 The sample was mounted in the Rudjer Boskovic Institute ion microprobe [15] and irradiated by
95 $18\ \text{MeV O}$ ions in a low current mode (up to 1000 counts per second (cps) at maximum). The
96 particular beam characteristics were chosen to fulfill the following requirements:

- 97 • The ions must traverse the entire sample to avoid polarization effect problems [16]
- 98 • Homogenous energy loss of ions throughout the depth of the sample, i.e., constant
99 electron-hole pair creation
- 100 • The total amount of deposited energy must be high enough to enable the use transient
101 current technique (TCT) [3] without the need for signal amplification and thus bandwidth
102 limitation.

103 According to SRIM [17] simulation the total energy deposition in a $3.25\ \mu\text{m}$ membrane of
104 traversing $18\ \text{MeV O}$ is approximately $10.78\ \text{MeV}$ with a homogenous profile, which corresponds

105 to a total amount of 830,000 electron-hole pairs (~133 fC) per ion. As a result of nearly
 106 homogenous e-h pair creation along the ion track, the contribution of electrons and holes to the
 107 induced signal is equal; therefore, it is not possible to distinguish the difference between their
 108 multiplication phenomena. The charge collection efficiency (CCE) of the detector was mapped by
 109 the Ion Beam Induced Charge (IBIC) technique [18]. The beam current was maintained at a very
 110 low level of 100-1000 cps. The signal was collected and amplified with a charge sensitive
 111 preamplifier (Ortec 142A), followed by a shaping amplifier (Ortec 570). Data acquisition was
 112 performed by Canberra 8075 ADC units and homemade software [19]. The scans at lower voltages
 113 were approximately 500x500 μm^2 in size to observe the response of the entire active detector area,
 114 including the electrode edges. At high electric fields, the scanning area was decreased to
 115 approximately 150x100 μm^2 (placed in the central part of the electrodes) to avoid hard breakdown
 116 at the electrode edges where the strength of the electric field can be enhanced, which is initiated by
 117 ion impact. The total bias spanned from -640 to +650 V, which corresponds to an electric field of
 118 ~200 V/ μm . This span of the electric field was greater than I-V measurements and eventually
 119 resulted in hard breakdown and microscopic bulk damage by the discharge at a bias of -650 V. The
 120 energy calibration of the measurement chain was performed with a silicon surface barrier detector
 121 and pulse generator. The CCE was calculated assuming an e-h pair creation energy of 13 eV [20]
 122 for diamond and 3.62 eV for silicon [21]. For the spectra recorded at different biases histograms
 123 were fitted with a Gaussian function and normalized to a calculated CCE. Figure 2. shows an
 124 overlap of the spectra at 100 V (~30 V/ μm , 100% CCE) and 600 V (185 V/ μm , proportional
 125 multiplication region). The position of the peak to the right corresponds to 2.2 times more collected
 126 charge, indicating the charge multiplication effect. The sigma of the peak is about 3 times larger,
 127 which is an indicator of higher statistical fluctuation because of the avalanching process [22].
 128 Figure 3. shows the dependence of the (CCE) versus the electric field strength (E) . The plot
 129 essentially consists of three parts. At low electric fields, 0-3 V/ μm in our case, the CCE is less than
 130 100% and follows the Hecht equation [23]. A CCE of 3-30 V/ μm asymptotically reaches 100% as
 131 expected and forms a plateau of almost constant efficiency. At higher electric fields, >30 V/ μm ,
 132 the CCE vs E dependence is exponential and exhibits a multiplication effect. According to McKay
 133 [24] and Chynoweth [25], the charge multiplication is parameterized by the multiplication factor
 134 α , the number of new e-h pairs produced per one charge per one micron. Because we cannot
 135 distinguish between holes and electrons, the α parameter is an average production value for both
 136 carriers. Following the derivation of McKay, a point charge, Q_0 , generated at one electrode results,
 137 after passing the thickness, d , of the detector, in a total charge Q equal to:

$$138 \quad Q = \frac{Q_0}{1 - \int_0^d \alpha x dx} \quad (1)$$

139
 140 In our experiment the beam traversed through the entire detector. The induced e-h pairs were
 141 uniformly distributed over the thickness of the detector, forming charge density per unit length
 142 instead of a point charge. However, the electric field was constant. Every e-h pair, generated

143 primarily at position x , creates αd new pairs before reaching end electrodes at 0 and d . These newly
 144 created pairs again have a chance αd to create new pairs. Therefore, after an infinite number of
 145 such calculations the following equation is obtained:

$$146 \quad Q = Q_0 + \alpha d Q_0 + (\alpha d)^2 Q_0 + \dots = Q_0 \sum_{i=0}^{\infty} (\alpha d)^i = \frac{Q_0}{1 - \alpha d} \quad (2)$$

147
 148 Here, no recombination is taken into account and 100% CCE is assumed on the plateau. The
 149 relationship between the α parameter and the electric field, E , can be empirically expressed in two
 150 ways. The first is to use the Chynoweth equation [25]:

$$151 \quad \alpha = a e^{-\frac{b}{E}} \quad (3)$$

152
 153 where a and b are fitting parameters. The second is to use the extended Chynoweth equation [4]:

$$154 \quad \alpha = a e^{-\frac{b}{(E)^c}} \quad (4)$$

155
 156 where the case of $c=1$ corresponds to (3). In some other semiconductors, the c parameter has been
 157 shown to be different than 1 [26]. There is no physical significance in the parameters a , b and c .
 158 Because the value of the c parameter in diamond is not established we fit the measured CCE to
 159 both (3) and (4): The fitting results are shown in Figures 3 and 4 and the parameters are listed in
 160 Table 1. Figure 3 shows that $c=0.2$ fit better represents high electric field, but it fails at low electric
 161 fields (visible also in Figure 4). Different slopes of the fits show a large freedom for the expected
 162 value of α at high electric fields. Figure 4 is the sum of all the theoretical and experimental work
 163 done in this area up to now. The measured multiplication parameter, α , for the highest measured
 164 electric field of $200 \text{ V}/\mu\text{m}$ in our experiment, equals approximately 1910 cm^{-1} and fits well between
 165 the two theoretical curves from [4, 12, 27]. However, extrapolation to the higher electric fields
 166 gives lower expectation than any other work for α parameter in that range.

a [μm^{-1}]	b [$\text{V}/\mu\text{m}$]	c
0.56 ± 0.03	216 ± 9	1
180 ± 31	19.7 ± 0.5	0.2

167
 168 Table 1.
 169 Fitting parameters for multiplication factor with two different equations

170 Equation (2) becomes divergent if $\alpha \times d = 1$. From this constraint, by extrapolation of the
171 measured α parameter, one may assume the avalanche breakdown (Geiger mode avalanche
172 threshold) field, where quenching is needed to stop the avalanching process. For the usual two-
173 parameter fit, as shown in equation (3), the calculation gives a threshold field of 363 V/ μm , whereas
174 the three-parameter fit (equation 4) gives a value of 285 V/ μm , for this 3.25 μm thick detector.

175 After reaching a hard breakdown for the charge sensitive measurements, the sample was
176 remetallized using a similar procedure as described above, again selecting a defect-free region. Due
177 to a number of defects and damage from previous breakdowns, the metallized area chosen was near
178 the edge of the etched part of the sample. The measured energy loss of the traversing ions through
179 the sample in this area was 15.1 ± 1 MeV which corresponds to about 4.25 ± 0.3 μm . To confirm
180 the sub-nanosecond avalanche process and exclude the photoconductive gain effect, we performed
181 a Transient Current Technique [3] measurement using only a bias TEE and Lecroy WaveMaster
182 8500; 5 GHz, 20 Gs/s digital storage oscilloscope. To protect the oscilloscope from damage, we
183 limited the bias span for the transient current measurements to 300 V, the value at which hard
184 breakdown is less probable and the multiplication process is evident from charge sensitive
185 measurements. The measured transient current signals are presented in Figure 5, where each trace
186 is an average of a few hundred single shots measured at 40V, 80V and 300V bias voltages. Even
187 at the lowest, 40 V bias (~ 9.4 V/ μm), the charge carrier velocities are almost saturated. Therefore,
188 any increase in current amplitude with bias increase is an indication of an avalanche multiplication.
189 However, because of the poor 50 ohm impedance matching, strong ringing of the signals was
190 observed. Taking into account the saturation velocity of both charge carriers ($1.2 - 2.7 \times 10^7$ cm/s)
191 [28] the intrinsic charge transit time was less than 40 ps for a 4.25 μm drift path. Such short signals
192 are quite challenging in terms of readout electronics and electrical connection bandwidth.
193 Approximately 18 GHz bandwidth would be needed to observe directly intrinsic transient current
194 signals, which was beyond the limits of the current experimental set-up. The 10-90% rise time of
195 all the signals was approximately 170 ps, corresponding to a 2 GHz bandwidth which is less than
196 the 5 GHz bandwidth of the digital storage oscilloscope. The observed bandwidth limitation is most
197 likely related to the inductance of the bonding wire connecting the upper contact and can be
198 improved in future experiments. Nevertheless, identical rise and fall times of all three signals and
199 progressively increasing amplitude, indicate a fast avalanching process related to the impact
200 ionization rather than photoconductive gain. The latter is the injection of charge carriers through
201 the ohmic contact in order to compensate the opposite charge that remained inside the device (due
202 to trapping and slower collection of one carrier) after the faster carrier is collected. The
203 photoconductive gain is proportional to the lifetime and inversely proportional to the transit time
204 of the charge carriers in the device, therefore it has a relatively long time constant, approaching the
205 life time of charge carriers in the tested material (a few ns in our case). More details about the
206 photoconductive gain mechanism can be found in [21] and photoconductive gain in diamond
207 detectors in [29]. The observed effect can find a practical application at the current stage in
208 detection techniques, i.e., time measurements with higher signal to noise ratio.

209

210 In conclusion, we have directly observed avalanche multiplication in a thin diamond detector.
211 Ionization coefficients were fitted to the experimental data and the minimum electric field for the
212 Geiger mode avalanche was determined. Compared to non-amplified signals, the TCT
213 measurements showed no long component of the multiplied signal related to photoconductive
214 gain, which supports the theory of an impact avalanche. The approach presented in this work
215 opens the possibility for the development of devices based on the avalanche principle as well as a
216 method to measure avalanche ionization coefficients for a better theoretical description of the
217 charge carrier transport in diamond material. Similar effect of charge multiplication is observed
218 on other diamond membranes, by irradiation with a number of different ion species. A more
219 detailed paper covering these is under preparation.

220

221 References

222 [1] A. Oh, *J. Inst.* 10, C04038 (2015)

223 [2] M. Pomorski, E. Berdermann, W. de Boer, A. Furgeri, C. Sander, and J. Morse, *Diamond*
224 *Relat. Mater.* 16, 1066 (2007)

225 [3] H. Pernegger, S. Roe, P. Weilhammer, V. Eremin, H. Frais-Kolbl, K. E. Griesmayer, H.
226 Kagan, S. Schnetzer, R. Stone, W. Trischuk, D. Twitchen, and A. Whitehead, *J. Appl. Phys.* 97,
227 073704 (2005)

228 [4] A. Hiraiwa, and H. Kawarada, *J. Appl. Phys.* 114, 034506 (2013)

229 [5] M. Suzuki, T. Sakai, T. Makino, H. Kato, D. Takeuchi, M. Ogura, H. Okushi and S.
230 Yamasaki, *Phys. Status Solidi A* 210, 2035 (2013)

231 [6] V. Mortet and A. Soltani *Appl. Phys. Lett.* 99, 202105 (2011)

232 [7] J. Isberg, M. Gabrysch, A. Tajani, and D. J. Twitchen, *Adv. Sci. Technol.* 48, 73 (2006)

233 [8] E. A. Konorova, Yu. A. Kuznetsov, V. F. Sergienko, S. D. Tkachenko, A. V. Tsikunov,

- 234 A. V. Spitsyn, Yu. Z. Danyushevskii, Sov. Phys. Semicond. 17, 146 (1983).
- 235 [9] M. Irie, S. Endo, C. L. Wang, T. Ito, Diam. Rel. Mat. 12, 1563 (2003).
- 236 [10] M. Pomorski, B. Caylar, and P. Bergonzo, Appl. Phys. Lett. 103, 112106 (2013).
- 237 [11] V. Grilj, N. Skukan, M. Pomorski, W. Kada, N. Iwamoto, M. Jakšić, T. Kamiya, Appl. Phys.
238 Lett. 103, 243106 (2013).
- 239 [12] T. Watanabe, M. Irie, T. Teraji, T. Ito, Y. Kamakura, and K. Taniguchi, Jpn. J. Appl. Phys.,
240 Part 2 40, L715 (2001).
- 241 [13] Element Six Ltd, King's Ride Park, Ascot, Berkshire SL5 8BP, UK
- 242 [14] <http://www.almax-easylab.com/>
- 243 [15] M. Jakšić, I. Bogdanović-Radović, M. Bogovac, V. Desnica, S. Fazinić, M. Karlusić, Z.
244 Medunić, H. Muto, Z. Pastuović, Z. Siketić, N. Skukan and T. Tadić, Nucl. Instrum. Methods
245 Phys. Res. B 260, 114 (2007).
- 246 [16] V. Grilj, N. Skukan, M. Jakšić, M. Pomorski, W. Kada, T. Kamiya, T. Ohshima, Nucl.
247 Instrum. Methods Phys. Res. B **372**, 161 (2016)
- 248 [17] www.srim.org
- 249 [18] M.B.H. Breese , E. Vittone , G. Vizkelethy, P.J. Sellin, Nucl. Instrum. Methods Phys. Res.
250 B 264, 345 (2007)
- 251 [19] M. Bogovac, I. Bogdanović, S. Fazinić, M. Jakšić, L. Kukec and W. Wilhelm, Nucl.
252 Instrum. Methods Phys. Res. B **89**, 219 (1994)

253 [20] L. S. Pan, S. Han, and D. R. Kania, *Diamond: Electronic Properties and Applications*.
254 Kluwer Academic, Dordrecht, 1995.

255 [21] G. F. Knoll, *Radiation Detection and Measurements*, Third Edition, John Wiley &
256 Sons, 2000

257 [22] R. J. McIntyre *IEEE Trans. Electron Devices*. 30, 164 (1966)

258 [23] K. Hecht, *Zeitschrift fur Physik*, 77, 235 (1932) [24] K. G. McKay, *Phys. Rev.* 94, 877 (1954)

259 [25] A. G. Chynoweth *Phys. Rev.* 109 1537 (1958)

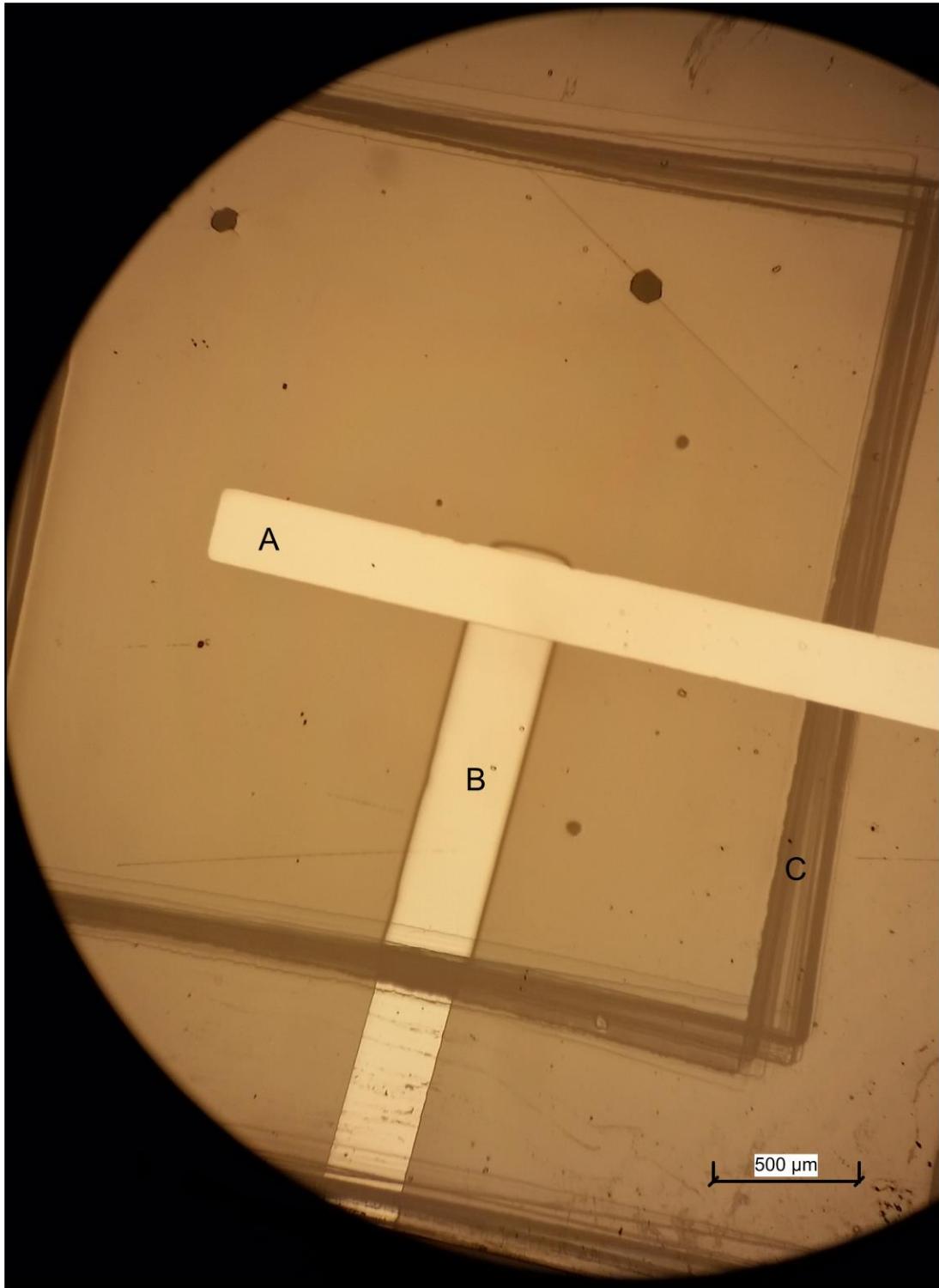
260 [26] F. Bertazzi, M. Moresco, and E. Bellotti, *J. Appl. Phys.* 106, 063718 (2009).

261 [27] A. Hiraiwa and H. Kawarada *J. Appl. Phys.* 117, 124503 (2015)

262 [28] M. Pomorski, *Doctoral Disertation*, Frankfurt 2008

263 [29] P. Bergonzo, R.B. Jackman (Chapter 6 authors), C. Nebel, J. Ristein (editors): *Thin-Film*
264 *Diamond II* Academic Press, 2004,

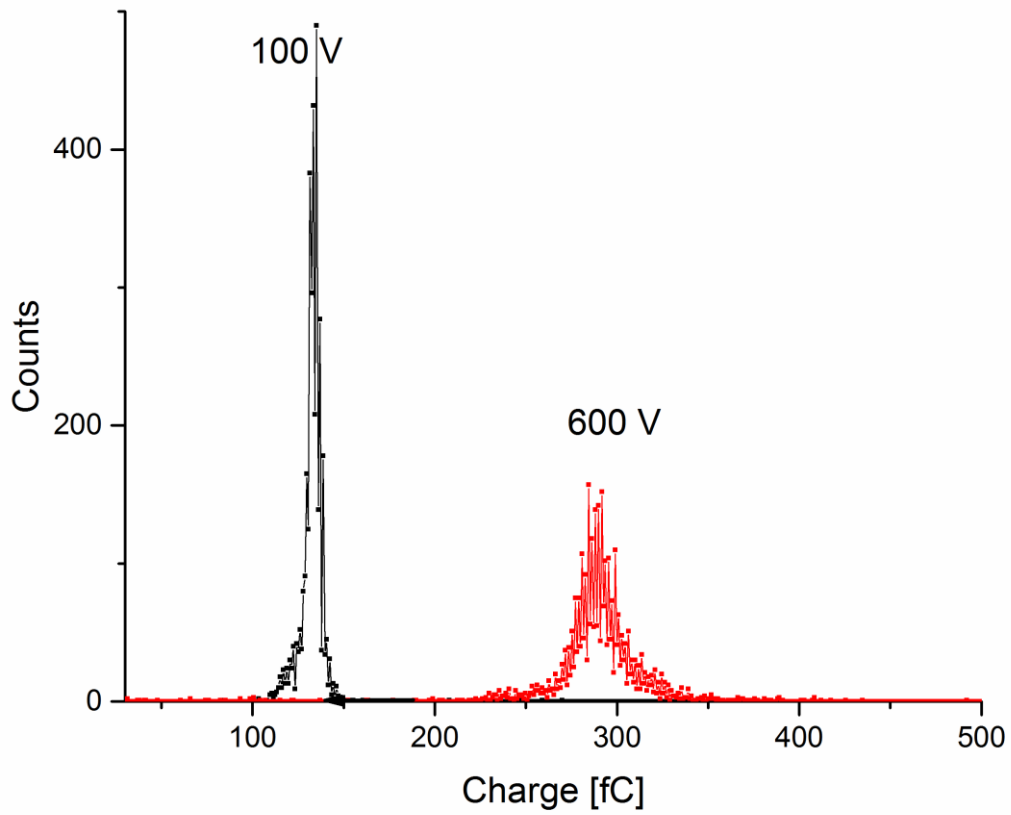
265



266

267 Figure 1. Microscope image of 3.25 μm thick scCVD diamond-membrane detector electrode
268 configuration. (A): upper electrode, (B): lower electrode, (C): the edge of the etched area

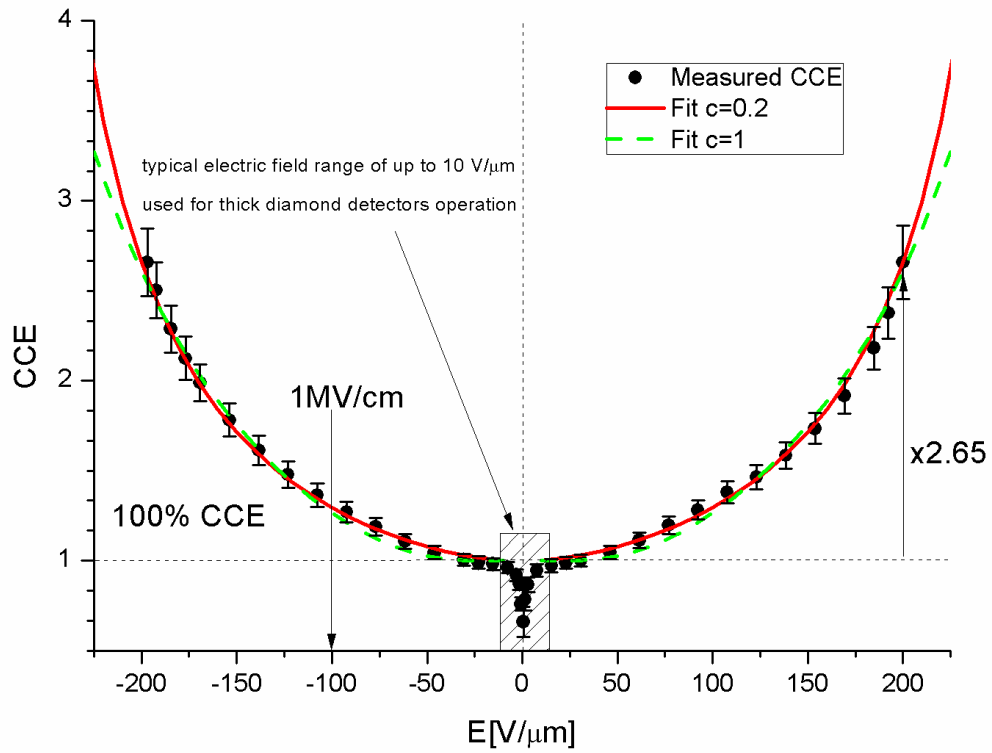
269



270

271 Figure 2. Measured energy loss spectra of 18 MeV O ion traversing the diamond-membrane.
272 100V bias voltage (30 V/ μm) and 600 V bias voltage (184 V/ μm). A $\times 2.2$ collected charge
273 multiplication is evidenced for the 600 V bias. The integral of both peaks is ~ 3500 counts.

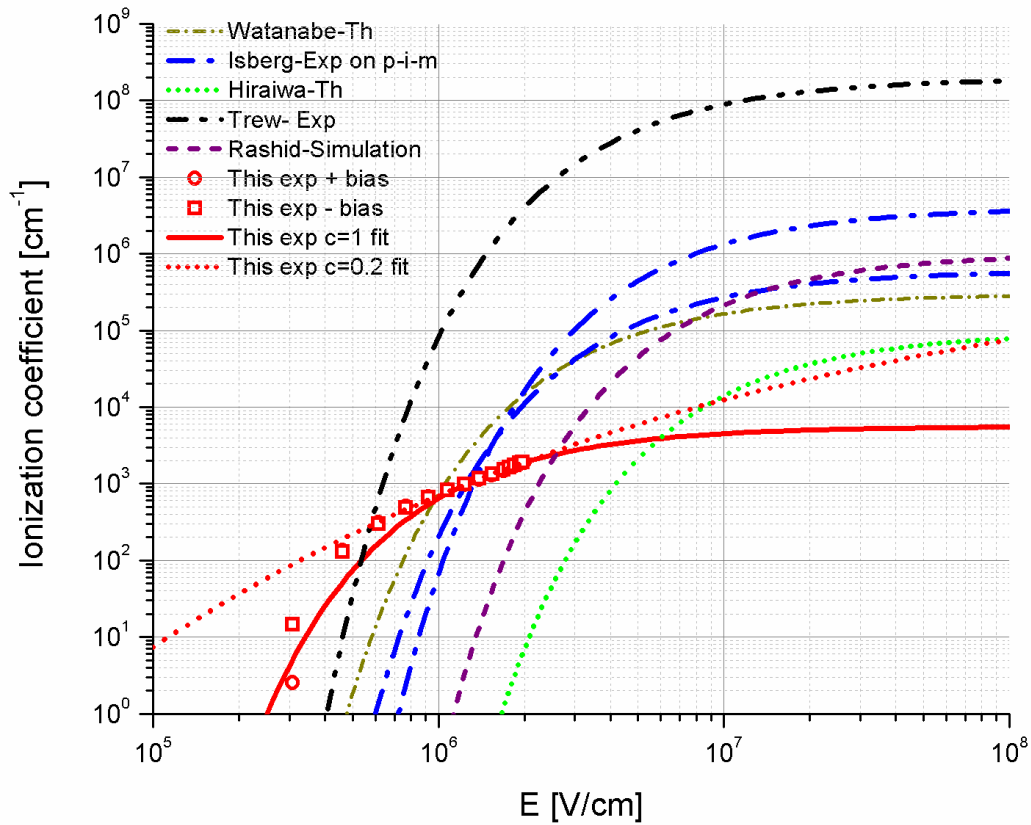
274



275

276 Figure 3. Electric field vs charge collection efficiency, where the black dots are measured
 277 points, the green line is a fit with the parameter $c=1$ and the red line represents fit with $c=0.2$.
 278 The patterned rectangular represent the typical range of operation for thick diamond detectors

279

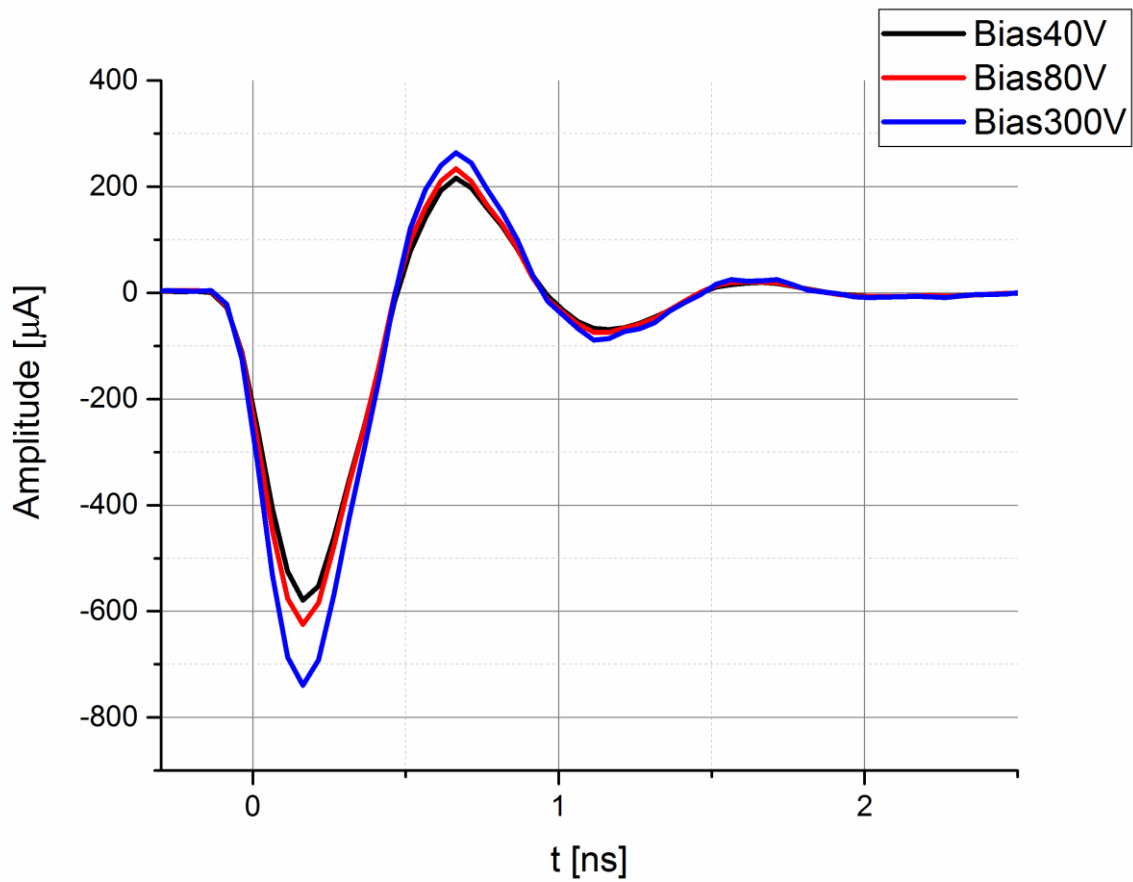


280

281 Figure 4. Comparison of α ionization parameter for different references and the present
 282 experiment. The solid red line represents the standard fit with $c=1$. The dashed red line is the
 283 fit with $c=0.2$. The data for the comparison were taken from [27] and references inside.

284

285



286

287 Figure. 5. Average over a few hundred single shots transient current signals for three different
 288 biases: 40V (9.4 V/μm-beginning of the 100% CCE plateau), 80 V (18.8 9.4 V/μm-plateau) and
 289 300 V (70.5 9.4 V/μm-multiplication regime). The curves are moved in time to better express
 290 equal shape of the traces.

291